FUDMA Journal of Engineering and Technology
ISSN: 3092-9385
https://fjet.fudutsinma.edu.ng/index.php/fjet/
Volume 2, Issue 1, 2026, 948-959

Characterisation of Pumice-Kaolin Refractory Bricks for High Temperature Industrial Applications

James AUDU[1*], Abdulraman A. SALAWU[2], Muriana R. AREMU[3], Abdullahi A. ALHAJI[4], Lawal S. SIUS[5]

[1*,4,5]Department of Mechanical Engineering, School of Infrastructure, Process Engineering and Technology, Federal University of Technology, Minna, Nigeria
[2,3]Materials and Metallurgical Engineering, School of Infrastructure, Process Engineering and Technology, Federal University of Technology, Minna, Nigeria

[1*]james.audu@st.futminna.edu.ng, [2]asipita.salawu@futminna.edu.ng, [3]mrraremu@futminna.edu.ng, [4]aliuaabdulla@futminna.edu.ng, [5]sadiq.lawal@futminna.edu.ng

Abstract

Pumice and kaolin refractory products are known to have outstanding resistance to thermal shock and high strength. However, knowledge about their optimization for better performance and sustainability is still not widely known. The objective of this study is to formulation and characterization of pumice-kaolin refractory bricks for its performance and sustainable properties in harsh industries. The refractory bricks were produced by mixing pumice (75-300 μm) and kaolin (150 μm) at ratios of 25:75, 50:50 and 75:25 and then fired at 1200 °C. Thermogravimetric Analysis (TGA), Differential Thermal Analysis (DTA), X-ray Fluorescence XRF analysis, Fourier-Transform Infrared spectroscopy (FTIR) were used to investigate the physico-mechanical, chemical and thermal properties of the samples. It was seen that alumina and silica were the major oxides with the porosity extent ranging from 24.2% to 71.4% which corresponds with the insulating refractory requirements. The highest porosity achieved was 75% pumice blend with excellent thermal shock resistance after repeated thermal cycles, flexural strength remained 87.56% retaining only 12.44% flexural strength loss. Each sample showed extremely high refractoriness, that is, the sample doesn't melt or deform even at 1200 °C, which satisfies the requirement of insulating bricks in industry. Based on these results, pumice-kaolin composites are considered as good raw materials for industry especially for ceramic applications as well as energy-intensive applications, due to their low cost and sustainability with good properties.

Keywords: *Refractory materials, Pumice, Kaolin, Refractoriness, High temperature.*

1.0 Introduction

The refractory materials are crucial for industrial processes which operate at high temperatures, such as the iron and steel industry, as they can endure the high temperatures without deteriorating, help maintain thermal stability and ensure structural strength under extreme conditions. These materials are those materials with chemical and physical properties applicable to structures exposed to environments above 538 °C [1], as stipulated by ASTM C71. Aluminosilicate refractories are the most widely used refractories, of which the major usage is in the iron and steel industry, accounting for about 70% of global refractory consumption [*2*]. Performance of various kinds of industrial processes is a direct function of refractory materials' performance and durability [*3*].

The current industrial requirement requires materials with high stability of mechanical properties under high temperature conditions, as well as high chemical stability. Current challenges are to develop greater thermal shock resistance, reduce the thermal conductivity for insulation use and increase the durability in harsh chemical conditions [*4*]. In addition, the industry has been paying increasing attention to finding cheaper, environmentally friendly refractory materials that use locally sourced materials [*5, 6*].

Pumice is a naturally occurring volcanic glass with unique characteristics which make it extremely appealing for low-density refractory applications. Experimental use of pumice coarse aggregate is found to be a low-density and high-porosity material, and the values obtained for the coefficient of thermal conductivity for the lightweight concrete are approximately 0.25–0.30 W/m·K, which is similar to the heat transfer of the material with control porosity [*7*]. Koyuncu *et al.*, [*8*], reported that the decomposition temperatures and the stability of the glass transition of the polymer systems containing pumice increased significantly.

The kaolin clay is a member of the aluminosilicate mineral group ($Al_2O_3 \cdot 2SiO_2 \cdot 2H_2O$) and is widely used in refractory construction due to its high silica and alumina content [*9*]. Kaolinite dehydroxylation by thermal treatment between 500-900 °C produces metakaolin which has an improved pozzolanic activity, which makes its reactivity and high-temperature applications more suitable [*9,10*]. When heating is carried out at temperatures higher than 1000 °C mullite crystallisation takes place and the crystallized mullite is a stable refractory phase which is similar with excellent thermal shock resistance and low coefficient of thermal expansion [*11*].

Received: 25/04/2026; Revised: 26/05/2026; Accepted: 29/05/2026; Published: 02/06/2026

In recent years, considerable research has been dedicated towards using natural pozzolanic material such as volcanic materials (pumice) as supplemental materials in high-temperature applications. Researches have shown that volcanic materials have considerable pozzolanic activity, which can be up to 22% in the course of time, which make them fit to use in industries [*12, 13*]. Advanced methods of improving kaolin ceramics by introducing additives in a nanostructured form have shown an increase in mechanical and thermal properties, providing a great deal of knowledge for applications in refractory industry [*14*].

While there is a substantial amount of research in the literature concerning the individual components, the research into pumice-kaolin composite for refractory is still limited. Refractory materials have been successfully produced in the past using alternative raw materials, with satisfactory mineral phases: cordierite, mullite and kyanite in the sintering temperature range of 1000-1200 °C [*15, 16*]. Thus, the purpose of this study is to create and characterise pumice-kaolin refractory bricks with differing ratios of pumice to kaolin at varying particle size for application at high temperature, in industry. The incorporation of pumice and kaolin in the formulations of the composite refractory materials has a great potential to achieve new and advanced materials that have the combined property of both materials which are highly porous, apt to excellent thermal insulation and the alumina-silica content gives the material a chemical stability and keeps it structurally sound.

2.0 Materials and Methods

2.1 Raw Materials

The pumice aggregates for this study were collected from Pati-Maga (Kutigi) in Niger State, Nigeria (9° 12' N, 5° 35' E) and the kaolin samples were collected from Ikere in Ekiti State, Nigeria (7° 30' N, 5° 14' E). The locations of the raw materials used are represented in Figure 1.

Figure 1: Sites of (A) pumice and (B) kaolin samples

The mining of pumice is an environmentally friendly extraction process, since it is an igneous rock that is deposited on the earth's surface in loose aggregate. Lump samples of kaolin were dug from a pre-existing open cast site. The samples were collected and mined from the locations depicted in Figure 1 by using diggers, cutlasses and hoes.

2.2 Sample Preparation

The pumice was dry processed by crushing, grinding, and sieving to prepare the pumice with different particle sizes of 75 μm, 150 μm and 300 μm. The kaolin samples were subjected to wet processing, which includes slurry preparation with water for 3 days to remove the harmful materials and sieving to be passed through a 150 μm mesh. The excess water in the soaked kaolin was then settled and decanted and the samples dried for 3 weeks at ambient temperature of 28 ± 2 °C. The dried kaolin samples were manually broken down into powder, and then ground and sieved through 150 μm mesh.

2.3 Brick Fabrication and Sintering

Refractory bricks were prepared using three particle sizes (75, 150, and 300 μm) and three weight percentages (25:75, 50:50, and 75:25) of the pumice and kaolin and thus nine different brick compositions were used, as shown in Table 1. Dry mixing of the mixtures was followed by moulding into cylindrical (100 × 50 mm), rectangular (100 × 20 × 20 mm) and conical shapes (57 × 20 mm) by hydraulic press and motor jack (Figure 2).

Table 1: Formulation of compositions of refractory samples

Samples	Sample code	Samples composition (%)		Particle size (μm)	
		Pumice	Kaolin	Pumice	Kaolin
1	A1	25	75	75	150
2	A2	50	50	75	150
3	A3	75	25	75	150
4	B1	25	75	150	150
5	B2	50	50	150	150

Received: 25/04/2026; Revised: 26/05/2026; Accepted: 29/05/2026; Published: 02/06/2026

Samples	Sample code	Samples composition (%)		Particle size (μm)	
		Pumice	Kaolin	Pumice	Kaolin
6	B3	75	25	150	150
7	C1	25	75	300	150
8	C2	50	50	300	150
9	C3	75	25	300	150

Figure 2: Refractory samples (A) produced and (B) standard cones

After being moulded and initially dried in the air for 48 h, samples were then dried under controlled conditions at 1300 °C in a gas-fired kiln with digital thermocouple temperature monitoring. The sintering schedule consisted of a slow firing to 450 °C for 4 hours. It was then heated to 1200 °C and held for 1 hour; and allowed to cool naturally inside the closed kiln.

2.5 Characterisation Techniques

2.5.1 Chemical Composition

The chemical composition of both pumice and kaolin samples was performed using an Energy Dispersive X-ray Fluorescence (EDXRF) at Umaru Musa Yar'adua University, Katsina with linear analysis technique to quantitatively determine their chemical compositions.

2.5.2 Thermal Analysis

The thermogravimetric analysis (TGA) and differential thermal analysis (DTA) were done at the same time on Federal University of Technology Minna with PerkinElmer TGA 400. Samples (10 ± 0.2 mg) were subjected to heating with a rate of 10 °C/min in the range from ambient temperature to 950 °C, with a nitrogen atmosphere of 20 mL/min.

2.5.3 Structural Characterisation

Happ-Genzel apodisation functions were used to determine the functional groups by Fourier-transform infrared (FTIR) spectroscopy. The samples were first dried and pulverized for the analysis. A small amount of each powder sample was poured onto the FTIR sample holder and scanned in the spectral range of 4000-650 cm-1 with a spectral resolution of 16 cm-1. The Happ-Genzel apodization function was employed during spectral acquisition to improve the spectral resolution and to reduce signal distortion. The spectra thus obtained were analysed with respect to the various functional groups and mineral phases present in the refractory materials.

2.5.4 Physical Properties

The physical properties were measured based on the ASTM C20 standard [17]. The bulk density (B) of the refractory samples was determined by burning the test samples of 35mm x 35mm, storing them in the oven and drying them to a constant weight; after drying, the oven - dry weight (D) of the samples is measured. Afterwards, the samples were saturated in water and the suspended weights in water (S) as well as the saturated weight in air (W) were measured. The bulk density (B) was calculated using equation 1:

$$B = \frac{D}{(W-S)} \quad [18] \tag{1}$$

where D= oven-dry weight (g), W =saturated weight in air (g), S=suspended weight in water (g).

The apparent porosity of the refractory samples was determined gravimetrically using Archimedes principle to measure open pore volume. The dried sample (D) was weighed and boiled in water to completely saturate the open pores. The soaked weight in air (W) and the suspended weight (S) in water were recorded to compute the total open pore volume using equation (2).

Received: 25/04/2026; Revised: 26/05/2026; Accepted: 29/05/2026; Published: 02/06/2026

$$Apparent\ porosity = \frac{W-D}{W-S} \times 100 \quad [18] \tag{2}$$

To determine the water absorption (WA), the refractory samples were oven-dry to achieve mass stabilization and the constant mass (M1 recorded. The samples were immersed in water for 24 hours at room temperature. The saturated surface dry sample was weighed as M2 and the samples were re-dried to a constant mass and weighed as M3. Water absorption (WA) was then calculated using Equation 3:

$$Water\ absorption\ (\%) = \frac{M2-M3}{M1} \times 100 \quad [18] \tag{3}$$

where M_2 = soaked weight, M_1= dry weight, M_3= the weight in air

The refractory samples were oven-dry to a constant mass and its dry weight in air recorded (D) to determine their apparent specific gravity (T). The samples were suspended in water to measure its submerged, apparent mass (S). Apparent specific gravity (ASG) was then determined using Equation 4:

$$T = \frac{D}{(D-S)} \tag{4}$$

where D= oven dry weight, S= suspended weight in water (ASTM C20) [17]

2.5.5 Mechanical Properties

The flexural strength of specimens of the untreated and treated pumice–kaolin composite was investigated to evaluate the ability of the samples to bend and the effect of the treatment on the mechanical properties of the samples. The test was performed following ASTM C1161 [19] procedure - Three-point bending method (Standard Test Method for Flexural Strength of Advanced Ceramics).

Rectangular test samples (150 x 25) mm have been prepared from both untreated and treated pumice–kaolin samples. All samples were molded, dried and sintered under controlled conditions before testing. The Three Point Bending Fixture was used in a Universal Testing Machine (UTM) to test the flexural strength of the samples. Two series of treated and untreated refractory specimens were prepared and placed horizontally on two rollers with fixed span length (e.g., 40 mm) and force was applied through a loading nose located in the center at a constant crosshead speed until the specimens fractured or yielded. The loading was incremented until the specimens failed. The maximum load at failure was automatically recorded by the testing software. This was done for each condition (treated and untreated) and the average was reported.

Thermal shock resistance was evaluated using a procedure based on ASTM C1171 [*20*] which requires repetitive thermal treatment of rectangular bar specimens. The percentage loss was determined by comparing the flexural strength after thermal shock to the original strength; not all thermal shock situations leads to a spalling or crack, but may lead to a weakness in the refractory. This structural weakness can manifest as weakness of the structure.

2.5.6 Refractoriness Testing

The Pyrometric Cone Equivalent (PCE) test was used to evaluate refractiveness, which is in accordance with ASTM C24 [*21*]. This test method involves forming a test piece (refractory cone measuring 57 x 20 mm) and comparing the deformation end point with a standard pyrometric cone. Cones were prepared from each of these compositions and were placed next to cones of standard composition (1000 °C, 1100 °C, and 1200 °C) on a pedestral and then heated until the cone was deformed. This is done to find out what the temperature would be at which each test sample would melt. The resulting PCE value is an indication of the refractoriness of the refractory material.

3.0 Results and Discussion

3.1 Material Characterisation

3.1.1 Chemical Composition

The chemical composition of both pumice and kaolin was analyzed by X-ray fluorescence (XRF) and is shown in Table 2, which indicates a total chemical composition of pumice equal to 47.37% SiO_2 and 15.68% Al_2O_3, while kaolin is equal to 46.04% SiO_2 and 24.35% Al_2O_3. This high alumina-silica content is a typical characteristic of good refractory materials, since the oxides form thermodynamically stable phases at high temperatures and offer excellent thermal stability and chemical resistance [11, *22*].

Received: 25/04/2026; Revised: 26/05/2026; Accepted: 29/05/2026; Published: 02/06/2026

Table 2: Chemical composition of the pumice aggregates and kaolin

Element	Concentration (%)	
	Pumice	kaolin
Fe_2O_3	8.1111	3.1750
SiO_2	47.374	46.041
Al_2O_3	15.684	24.354
MgO	1.69	0.97
P_2O_5	0.4150	0.0013
SO_3	0.1321	11.79
TiO_2	1.6221	0.5808
MnO	0.2810	0.00678
CaO	5.238	0.03426
K_2O	1.717	0.0944
CuO	0.00277	0.00596
ZnO	0.01788	0.00728
Cr_2O_3	0.00341	0.00540
V_2O_5	0.0984	0.0329
PbO	0.6097	0.0858
Rb_2O	0.00255	0.00170
NiO	0.01773	0.00766
Cl	0.0187	0.066
ZrO_2	0.4098	0.4663
Ta_2O_5	0.0106	0.0287
WO_3	0.1179	0.1107
Nb_2O_5	0.5112	0.5054
Cs_2O	0.23	0.23
Sb_2O_3	0.115	0.156
CeO_2	0.134	0.484
SrO	0.542	0.2650
Au	0.0017	0.0010

With the presence of other oxides, e.g. Fe_2O_3, CaO and K_2O in small amounts, the sintering behaviour and the properties of the refractory bricks can be affected. It has been demonstrated that amorphous aluminosilicates and particle size distribution have profound effects on the reactivity of pumice [*8*, *23*].

3.1.2 Thermal Behaviour

The TGA analysis of the pumice aggregates showed a multi-stage thermal degradation of the material as shown in Figure 3. The curve of the pumice sample shows that its mass loss was steady up to the onset temperature as mentioned in the Figure. 3 [[*24*].]. The TGA curve showed a slow decrease in mass from ambient temperature to around 270 °C, which was thought to be due to the evaporation of physically adsorbed water. The thermal decomposition of pumice was carried out in three stages (Table 3) as expected for an amorphous material.

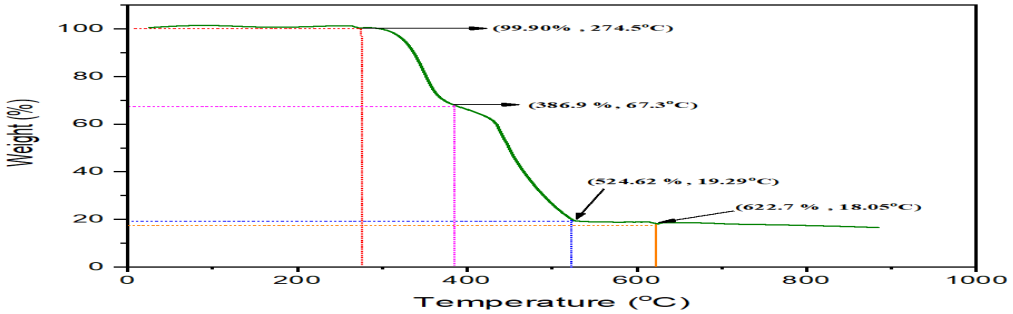

Figure 3: TGA Curve for pumice aggregates

Stage 1 (274.5 °C) was attributed to the complete removal of moisture trapped on the surface of the sample. Stage 2 (386.9-524.6 °C) had progressive mass loss of around 48% probably due to the decomposition of organics and dehydroxylation of hydroxylated aluminosilicates. The results of the stage 3 (622.7 °C) showed the total

degradation with a residual weight of 18.05%, which is excellent thermal stability for high temperature applications [25]. This means that the pumice is volatile constituents and hydroxyl-bearing aluminosilicate phases and that it is only stable above 650 °C. The results of this TGA profile suggest that the material could be used as a light weight insulating refractory material after being decomposed. The intermediate mass loss of 48% may come from highly hydrated phases and high volatile or organic content, suggesting preheating or calcination treatment prior to using it as a refractory to enhance thermal stability and service performance at high temperatures [26]. The decomposition of the possible constituents in the refined pumice sample, as demonstrated in Table 3 caused the degradation temperatures to change.

Table 3: Degradation temperature of pumice aggregates

S/N	Weight (%) Loss	Degradation Temperature (°C)
1	99.90	274.5
2	67.30	386.9
3	19.29	524.6
4	18.05	622.7

The TGA curve for kaolin (Figure 4) showed three distinct mass loss regions as given in Table 4, which is typical of kaolinitic clays. The first stage (162 °C) revealed a small loss of weight (0.027%) that was due to physically adsorbed water. The 0.49% mass loss at the stage 2 (340 °C) was also ascribed to a progressive dehydroxylation initiation. Stage 3 (599.4 °C) showed considerable mass loss (4.00%), consistent with the complete dehydroxylation of kaolinite as follows: $Al_2Si_2O_5(OH)_4 \rightarrow Al_2Si_2O_7$ (metakaolin) + $2H_2O$, a reaction that has been well documented and typically occurs between 450-650 °C [27, 28]. The thermal stability values (Table 4) represent the temperatures at which kaolin lost the percentage of its mass: 96% at 303 °C, 88% at 494 °C and 20% at 716 °C, which are in agreement with earlier work [29, 30].

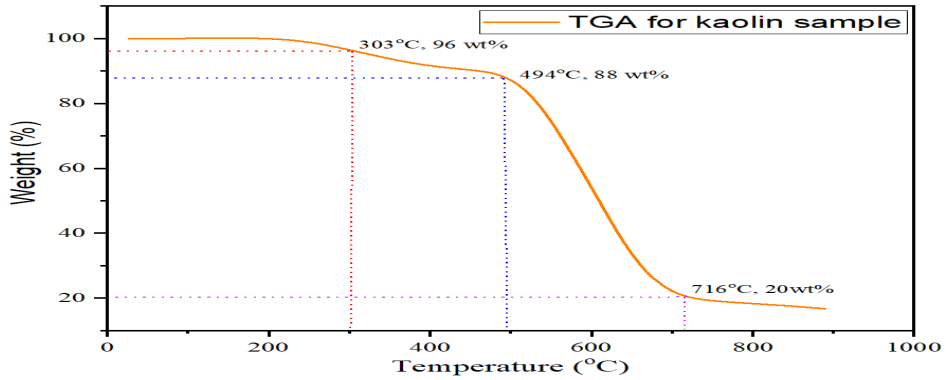

Figure 4: TGA Curve for Kaolin sample

Table 4. Thermal stability values of kaolin sample

S/No	Weight (%) loss	Stability Temperature (°C)
1	96	303
2	88	494
3	20	716

3.1.3 Structural Characterisation

The Fourier-transform infrared (FTIR) spectroscopy analysis of the pumice samples yielded characteristic absorption peaks at 745, 922, 997, 1295, and 1424 cm-1, corresponding to different modes of vibration such as Si-O-Si symmetric stretching (745 cm-1), Na-OH bending (922 cm-1), Si-O asymmetric stretching (997 cm-1), C-O stretching (1295 cm-1), and Ca-O vibrations (1424 cm-1) as seen in Figure 5.

Received: 25/04/2026; Revised: 26/05/2026; Accepted: 29/05/2026; Published: 02/06/2026

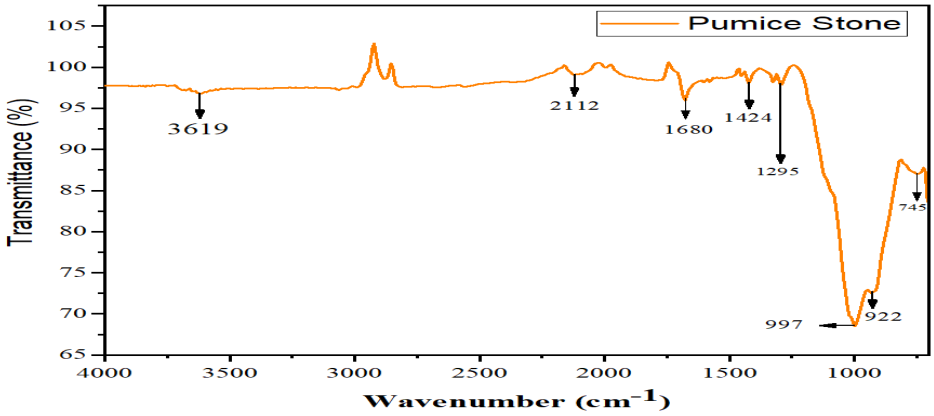

Figure 5: FTIR Spectra for pumice stone

A wide band of absorption around 3200-3600 cm^{-1} was suggestive of the presence of O-H stretching of hydroxyl groups and molecular water. These spectral features are in excellent agreement with previously reported results [31, 32], confirming the predominantly aluminosilicate composition which are essential for thermal stability and refractory performance with minor carbonate and hydroxide phases. The comparison with the previous studies has just been confirmed and proves the mineralogical reliability and consistency of pumice thus making it suitable for use as a lightweight aluminosilicate raw material in insulating refractory applications.

3.2 Refractory Properties

3.2.1 Physical Properties

The complete physical properties of the nine compositions of sintered refractories are shown in Figure 6. Sample B3 with pumice content 75% and Kaolin 25%, and with average diameter of 150μm had the highest apparent porosity of 71.40%, which was much higher than the minimum requirement of insulating refractory bricks, which is 40% [33]. This is an extraordinarily high porosity that is attributed to the inherent porosity of pumice particles as well as inter-particle porosity formed in the course of sintering. Sample A2 (50% pumice, 50% kaolin, 75 μm) had the lowest porosity (24.20%), which could be explained from the better particle packing efficiency achieved by using finer pumice particles with higher kaolin amount to increase the densification. The porosities of samples A1 (43.30%), B2 (46.90%), B3 (71.40%) and C1 (58.80%) were within the range of 40-85% required for insulating refractory bricks [32] which indicates their thermal insulation property. The porosity, water absorption, specific gravity and bulk density are represented by P(%), A(%), T and B respectively in Figure 6.

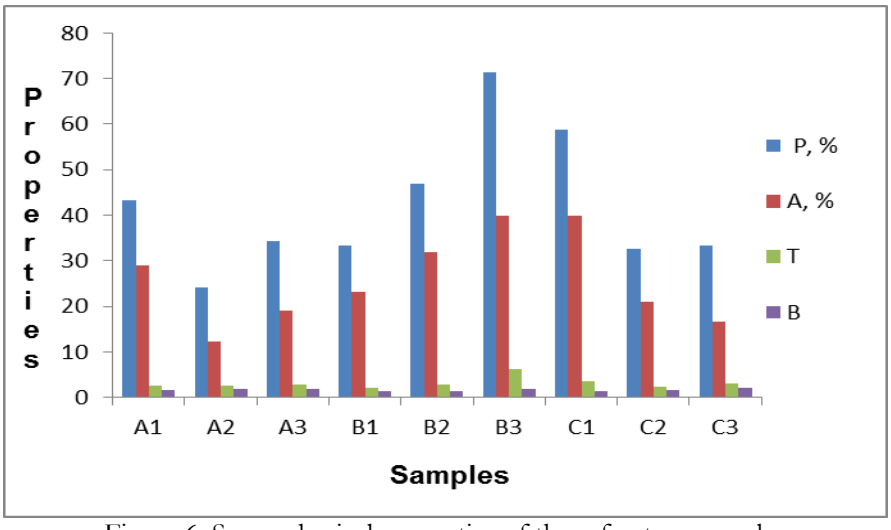

Figure 6: Some physical properties of the refractory samples

The water absorption showed an inverse relationship with the bulk density with the most water absorption having the lowest bulk density and hence the lowest porosity represented by sample A2. This property is indicative of greater durability and better resistance to attack in service environments. The bulk density of the compositions varied between around 1.1 g/cm^3 (highest porosity) and 1.9 g/cm^3 (lowest porosity), which is typical for insulating refractories (0.8-2.0 g/cm^3) [34]. The apparent specific gravities were between 2.4 and 2.7, which is the intrinsic density of solid aluminosilicate phases.

Received: 25/04/2026; Revised: 26/05/2026; Accepted: 29/05/2026; Published: 02/06/2026

The flexural strength tests showed that the fine particle size pumice (group A) has higher strength for all pumice-kaolin mixing ratios. The flexural strength of the untreated samples is shown in Figure 7 while the thermal shock treated samples are shown in Figure 8. Not all situations of thermal shock result in spalling or cracking, but may result in structural weakness of the refractory which is evident from the loss of strength. Thus, the modulus of the treated specimens was compared to that of the untreated specimens. The flexural strength for all the specimens showed a decrease to a certain extent. The flexural strength of the sample A3 (75% pumice, 25% kaolin, 75 μm) is not affected by the thermal cycling, the sample is still excelling in thermal shock resistance, maintaining 87.56% of its original flexural strength after thermal cycling, which is equivalent to strength loss of 12.44% (Figure 9). This could be explained by the synergistic effect of fine particle size, optimized porosity, strong bonding of aluminosilicate within the refractory composite and reduced thermal stress development in the composite. The higher the porosity, the better the water absorbed and the lower the mechanical strength [35, 36]. The flexural strength retention after thermal cycling was 87.56%, which shows minimal damage to the material in terms of thermal damage, propagation of microcracks, or degradation in the material structure while exposed to rapid temperature changes. In general, it can be concluded that the material possess good mechanical integrity and performance under repeated thermal exposure.

Figure 9 shows that the method applied increased the strength of the material, suggesting that surface defects were reduced and microstructural cohesion was enhanced, allowing for better stress transfer within the material. This finding is in line with the work by Celik and Urtekin, (2025) [37] who reported that steel-basalt hybrid fibre concretes exhibited notable enhancements in flexural properties following high-temperature exposure and re-curing, which was mainly attributed to the increased bonding and crack-bridging mechanisms. In the same way, Li et al. (2022) [38] and Wei et al. (2024) [39] presented the effect of the surface or matrix modification of alumina ceramics on flexural strength which could reach as high as 37%.

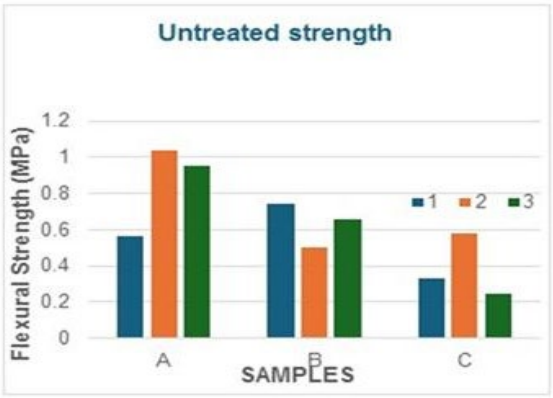

Figure 7: Untreated strength

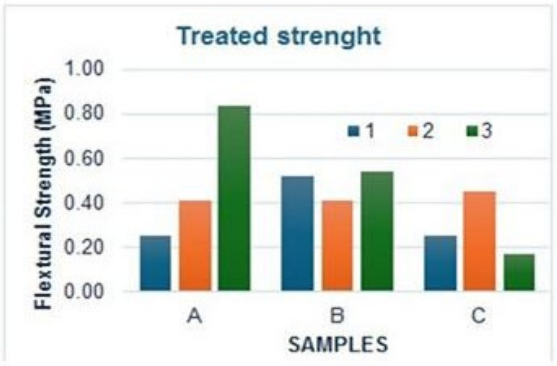

Figure 8: Treated strength

The high thermal insulation properties due to high pumice content, low thermal gradients, small particle size and good porosity due to inclusion of thermal expansion and contraction were responsible for this outstanding performance [33, 40]. Figure 9 shows that after thermal shock cycles, the loss in strength increases, whereas in case of flexural strength at ambient temperature, as shown in Figure 10, the flexural strength of samples is more or less equal.

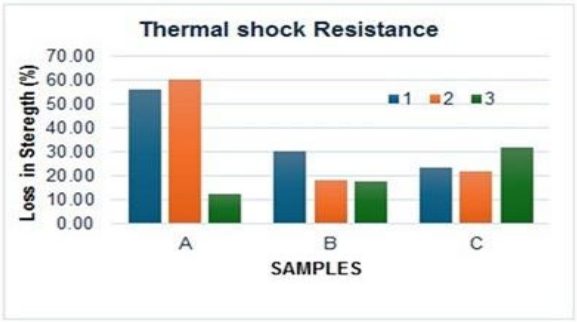

Figure 9: Loss in strength after exposure to thermal shock cycles

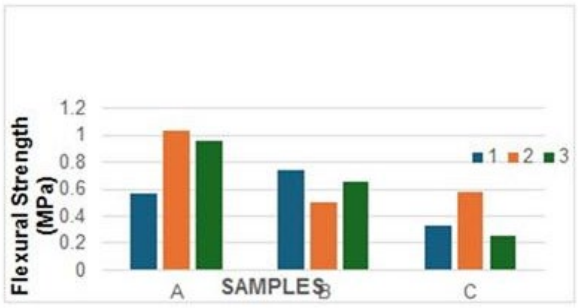

Figure 10: Flexural strength of samples at ambient temperature

The synergistic mechanisms responsible for the superior thermal shock resistance of the pumice-rich compositions are: high porosity decreasing elastic modulus and thermal conductivity, which decreases the generation of thermal stress; microcrack toughening due to pre-existing flaws that act as natural crack intercepting

sites and cause cracking to deflect; and mitigation of the thermal gradients due to the low value of thermal conductivity [41]. The results from this study are compared to the data on literature for commercial insulating refractories and they are comparable with the typical values of thermal shock as reported for the clay based insulating firebricks [18].

3.2.3 Refractoriness

The Pyrometric Cone Equivalent (PCE) tests showed that none of the compositions melted, slumped or significantly deformed up to 1200 °C (Figure 11). Based on this outstanding performance, it is inferred that the actual refractoriness of the developed composites is greater than 1200 °C as there is no melting or deformation at 1200 °C. An excellent refractoriness is explained by the high alumina-silica content (63-70%) which gives rise to refractory oxide phases, mullite (melting point ~1850 °C) and cristobalite (melting point ~1710 °C) during sintering [42 ,43].

Figure 11: Showing standard cones squatting while test samples remain standing

The above 1200 °C refractoriness makes these pumice-kaolin composites suitable for various industrial uses such as furnace lining, insulating material in kiln, metallurgical and ceramic industries in which the property of moderate to high thermal resistance, lightweight structure and insulation is required.

3.2 Implications for Industrial Applications

The study of industrial implications and comparison will be conducted in this section. The pumice-kaolin refractory bricks possess high porosity, strong mechanical properties, excellent thermal shock resistance and high refractoriness, thus they are suitable for a wide range of industrial applications with high temperatures. Such materials are especially suitable for furnace lining, Insulation of the furnace for the metallurgical and ceramic industries, as well as thermal insulation applications. The flexibility is owed to the fact that its properties can be varied by manipulating the ratio of pumice to kaolin and the particle size of the pumice, depending on the specific requirements of the industry, so that it could be used accordingly to achieve a higher porosity for better thermal insulation or a finer pumice particle size for better mechanical properties.

The performance of the developed refractory bricks is verified by benchmarking with commercial bricks, showing that several parameters meet or exceed standards. Samples A1, B2, B3 and C1 that have porosities greater than 40% are in line with the standards set for the insulation refractories by industry [32]. High refractoriness resisting temperature of 1200 °C and strength loss of 12.44% are signatures of excellent thermal shock resistance which is similar to high quality commercial insulating bricks. These features, along with the use of local natural resources, are significant benefits such as low cost, lower carbon footprint due to the elimination of long-distance transportation, sustainability of the resources and possible regional economic benefit.

4.0 Conclusion

In this study, the feasibility of developing pumice-kaolin based insulating refractories having a desired thermo-mechanical property by systematic control of composition, particle size and processing conditions was successfully demonstrated. The chemical analysis of the samples of the pumice and kaolin revealed aluminium oxide (Al_2O_3) and silica (SiO_2) as major components indicating its suitability to be used as aluminosilicate refractory material. Apparent porosity varies from 24.2% to 71.4% and four compositions are found to meet the industrial requirement of 40-85% porosity for an insulating refractory. It was found that the porosity increased from about 24% to more than 70% significantly with the increase of pumice content from 25% to 75% of the mixture, whereas

Received: 25/04/2026; Revised: 26/05/2026; Accepted: 29/05/2026; Published: 02/06/2026

bulk density decreased from about 2.0 g/cm³ to 1.4 g/cm³, which resulted in a significant increase in thermal insulation capability and a reduction of mechanical strength. The flexural strength was found to be reduced by more than 40% at higher amounts of pumice, reflecting the balancing act between insulation properties and strength. From the overall results, it may be concluded that the experimental analyses showed that the replacement of sand by pumice up to 80% is necessary rather than the maximum replacement to get the desired performances and high refractoriness was observed for all matrix composition without any melting or deformation up to 1200 °C.

The use of these locally available and economical raw materials represents a potential avenue for developing more sustainable and economic refractory materials for high-temperature applications in industry. Future research should include long-term durability testing under simulated industrial environments, optimizing production processes for large scale production, investigating using supplementary additives to further improve specific properties and life cycle assessment to quantify the environmental benefits. These results demonstrate that the pumice-kaolin composites are technically feasible, economically attractive and environmentally friendly refractory materials for energy intensive industries, especially for developing nations, where volcanic pumice and kaolin deposits are available.

Acknowledgment

The authors are thankful to Scientific Equipment Development Institute (SEDI), Minna and Federal University of Technology, Minna, Nigeria, under the Department of Mechanical Engineering for their financial support and research facilities. Laboratory technical assistance is much appreciated.

References

[1] ASTM C71, "Standard terminology relating to refractories," ASTM International, vol. 15 no. 1, pp. 1-12, 2020, https://doi.org/10.1520/C0071-18

[2] H. H. Murray, "Applied clay mineralogy: occurrences, processing and application of kaolins, bentonites, palygorskite-sepiolite, and common clays," in Developments in Clay Science, vol. 2, Amsterdam, The Netherlands: Elsevier, 2006, pp. 1–180.

[3] V. O. Chinwuba and M. S. Uzoma, "Optimisation of blast furnace throughput based on hearth refractory lining and shell thickness," Journal of Casting and Materials Engineering, vol. 5, no. 1, pp. 5–13, 2021. Available: https://doi.org/10.7494/jcme.2021.5.1.5

[4] V. Diana, "Thermo-physical properties of insulating refractory materials," Ph.D. dissertation, Univ. Limoges, Limoges, France, 2021, pp. 1-117.

[5] A. Zharmenov, S. Yefremova, B. Satbaev, N. Shalabaev, S. Satbaev, S. Yermishin, A. Kablanbekov, "Production of refractory materials using a renewable source of silicon dioxide," Minerals, vol. 12, no. 8, 2022, Art no. 1010, https://doi.org/10.3390/min12081010

[6] M. M. Dansarai, M. A. Bawa, and A. Tokan, "Nigerian clay deposits for use as refractory materials in metallurgical industries – A review," Int. J. Eng. Res. Technol., vol. 9, no. 6, pp. 707–711, Jun. 2020, doi: 10.17577/IJERTV9IS060520.

[7] M. Tuncer, A. Bideci, Ö. S. Bideci, B. Çomak, and G. Durmuş, "Engineering properties and thermal conductivity of lightweight concrete with polyester-coated pumice aggregates," Science and Engineering of Composite Materials, vol. 32, no. 1, p. 20250057, 2025.

[8] M. Koyuncu, G. Ulay, and U. Şeker, "Effect of pumice powder on mechanical, thermal, and water absorption properties of fiberboard composites," Fibres & Textiles in Eastern Europe, vol. 31, no. 3, pp. 30–36, 2023. https://doi.org/10.2478/ftee-2023-0025

[9] M. Valaskova, "Clays, clay minerals and cordierite ceramics – A review," Ceramics–Silikáty, vol. 59, no. 4, pp. 331–340, 2015.

[10] J. R. T. Reddy, J. Schuster, and Y. P. Shaik, "Development of kaolin and glass fiber reinforced composites for thermal insulating panels," Open J. Compos. Mater., vol. 14, no. 1, pp. 44–59, 2023.

[11] M. Garcia-Valles, P. Alfonso, S. Martínez, and N. Roca, "Mineralogical and thermal characterisation of kaolinitic clays from Terra Alta (Catalonia, Spain)," Minerals, vol. 10, no. 2, pp. 1–15, 2020, Art. no. 142.

[12] F. J. Jubera-Pérez, E. Jaizme-Vega, R. Rosa-Orihuela, R. Damas-Montesdeoca, C. Hernández-Díaz, J. Rodríguez-Díaz, and E. González-Díaz, "Pozzolanic activity of volcanic ashes produced by the eruption of the Tajogaite Volcano in La Palma, Canary Islands," Construction and Building Materials, vol. 419, p. 135498, 2024. [Online]. Available: https://doi.org/10.1016/j.conbuildmat.2024.135498

[13] J. Rosales, M. Rosales, J. L. Díaz-López, F. Agrela, and M. Cabrera, "Effect of processed volcanic ash as active mineral addition for cement manufacture," Materials, vol. 15, no. 18, p. 6305, Sep. 2022. [Online]. Available: https://doi.org/10.3390/ma15186305

[14] N. A. M. Barakat, N. A. M. Eltohamy, K. R. M. Abdelrazek, W. Elhawam, A. A. A. Ammar, H. Fouad, "Advanced strategies for enhancing kaolin ceramics using nanostructured additives: A comprehensive study," PLoS ONE, vol. 20 no. 5, 2025. https://doi.org/10.1371/journal.pone.0324449

[15] K. Belbali, A. Loucif, J. Tamayo, and F. Rubio, "Influence of heating temperatures on structure and microstructure of chamotte-carbon composites," Boletín de la Sociedad Española de Cerámica y Vidrio, vol. 61, no. 2, pp. 54–63, 2022

[16] S. Kamara, W. Wang, and C. Ai, "Fabrication of refractory materials from coal fly ash, commercially purified kaolin, and alumina powders," Materials, vol. 13, no. 15, p. 3406, 2020. [Online]. Available: https://doi.org/10.3390/ma13153406

[17] ASTM C20-00, "Standard test methods for apparent porosity, water absorption, apparent specific gravity, and bulk density of burned refractory brick and shapes by boiling water," ASTM International, West Conshohocken, PA, USA, 2015, doi: 10.1520/C0020-00R15.

[18] V. E. Ojukwu, R. O. Ajemba, "The effect of sawdust, cow dung, and CaC_2 wastes on properties of refractory bricks," Journal of Engineering and Applied Sciences, vol. 21, no. 1, pp.799–812, 2022.

[19] ASTM International, AASTM C1161-18(2023): Standard Test Method for Flexural Strength of Advanced Ceramics at Ambient Temperature, West Conshohocken, PA, USA, 2023.

[20] ASTM International, ASTM C1171-16(2022), Standard Test Method for Quantitatively Measuring the Effect of Thermal Shock and Thermal Cycling on Refractories, West Conshohocken, PA, USA, 2022. doi: 10.1520/C1171-16R22.

[21] ASTM C24, "Standard Test Method for Pyrometric Cone Equivalent (PCE) of Fireclay and High-Alumina Refractory Materials," ASTM International, 2001, pp. 1–5.

[22] A. Olalere, S. S. Yaru, and O. A. Dahunsi, "Evaluation of the chemical and thermo-physical properties of locally aggregated kaolin-based refractory materials," *Journal of Mechanical Engineering and Sciences*, vol. 13, no. 1, pp. 4743–4755, 2019.: https://doi.org/10.15282/jmes.13.1.2019.27.0397

[23] R. M. Khattab, A. H. Abdel-Aziem, M. A. Wahba, "Synthesis and characterization of kaolin glass cullet nanocomposites," Scientific Reports, vol. 15 Art no.10453, 2025. https://doi.org/10.1038/s41598-025-03908-6

[24] E. Lalla, A. Sanz-Arranz, G. Lopez-Reyes, M. Konstantinidis, and F. Rull, "A micro-Raman and X-ray study of erupted submarine pyroclasts from El Hierro (Spain) and its astrobiological implications," *Life Sci. Space Res.*, vol. 21, pp. 49-64, May 2019

[25] A. Shoroog, A. Hasan, "Physical properties of mesoporous scoria and pumice volcanic rocks," Journal of Physics Communications, vol. 5, pp. 1–15, 2021, https://doi.org/10.1088/2399-6528/ac3a95

[26] F. Zunino and K. Scrivener, "Reactivity of kaolinitic clays calcined in the 650–1050 °C temperature range: Towards a robust assessment of over-calcination," Cement and Concrete Composites, vol. 146, p. 105380, 2024, doi: 10.1016/j.cemconcomp.2023.105380.

[27] A. A. Ayalew, "Physiochemical characterisation of Ethiopian mined kaolin clay through beneficiation process," Advances in Materials Science and Engineering, vol. 2023, no. 1, pp. 1–8, 2023, https://doi.org/10.1155/2023/9104807

[28] Y. Wang, L. Hu, Z. Yin, "Identification and quantification of soil water components in kaolin by thermogravimetric and kinetic analyses," Engineering Geology, vol. 324, art no. 107273, 2023, https://doi.org/10.1016/j.enggeo.2023.107273

[29] F. Zunino, K. Scrivener, "The reaction between metakaolin and limestone and its effect in porosity refinement and mechanical properties," Cement and Concrete Research, vol. 140, art no. 106307, 2021, https://doi.org/10.1016/j.cemconres.2020.106307

[30] B. Ersoy, A. Sariisik, S. Dikmen, G. Sariisik, "Characterisation of acidic pumice and determination of its electrokinetic properties in water," Powder Technology, vol. 197, pp. 129–135, 2010, https://doi.org/10.1016/j.powtec.2009.09.005

[31] P. H. Chang, Z. Li, J. S. Jean, W. T. Jiang, C. J. Wang, and K. H. Lin, "Adsorption of tetracycline on 2:1 layered non-swelling clay mineral illite," Applied Clay Science, vol. 67–68, pp. 158–163, 2012. [Online]. Available: https://doi.org/10.1016/j.clay.2011.11.004

[32] R. Kumar, Development of low bulk density fireclay insulation brick, B.Tech. thesis, Department of Ceramic Engineering, National Institute of Technology. Rourkela, India, 2011, pp. 1–26.

[33] J. B. Mokwa, S. A. Lawal, M. S. Abolarin, and K. C. Bala, "Characterization and evaluation of selected kaolin clay deposits in Nigeria for furnace lining application," Nigerian Journal of Technology *(NIJOTECH)*, vol. 38, no. 4, pp. 936–946, 2019, doi: 10.4314/njt.v38i4.17.

[34] "Lightweght Insulating Refractory Materials," Refractory Furnace. [online]. Available: https://refractoryfurnace.com/. Assessed: May 23, 2026.

[35] F. Mobasheri, A. A. J. Shirzadi, S. Mirvalad, S. Azizi, and R. Mowlaei, "Durability and mechanical properties of pumice-based geopolymers: a sustainable material for future," Iranian Journal of Science and Technology, Transactions of Civil Engineering, vol. 46, no. 1, pp. 223–235, 2022.

[36] K. Moolchandani, "Advancements in pumice-based concrete: A comprehensive review," Next Materials, vol. 8, no. 1, pp. 1-13, 2025. doi: https://doi.org/10.1016/j.nxmate.2025.100646.

[37] Z. Celik and Y. Urtekin, "Effects of High Temperature and Water Re-Curing on the Flexural Behavior and Mechanical Properties of Steel–Basalt Hybrid Fiber-Reinforced Concrete," Applied Sciences, vol. 15, no. 3, p. 2076, 2025.

[38] H. Y. Li, H. Hao, Y. Tian, X. G. Liu, D. Wan, and Y. Bao, "Temperature dependence of flexural strength and residual stress of \(Al_{2}O_{3}\) reinforced by kyanite coating," Ceramics International, vol. 48, no. 19, pp. 28745-28750, 2022.

[39] H. Wei, Y. Li, Y. Sun, K. Li, Y. Bao, & D. Wan, "A novel prestress strategy to improve thermal shock resistance of bone china body," Journal of the Australian Ceramic Society, vol. 60, no.2, pp. 619-628, 2024.

[40] O. Oyebanjo, G. Ekosse, J. Odiyo, Physico-chemical, mineralogical, and chemical characterisation of Cretaceous–Paleogene/Neogene kaolins within Eastern Dahomey and Niger Delta Basins from Nigeria: Possible industrial applications, Minerals 10 (2020) 670. https://doi.org/10.3390/min10080670

[41] M. I. Hussain and Z. Chen, "Multi-objective optimization and performance evaluation of refractory materials for high-temperature industrial furnaces," Journal of Advanced Materials Science, vol. 12, no. 3, pp. 234–248, 2024. [Online], https://doi.org/10.1177/1687813225134623

[41] M. I. Hussain, Z. Chen, Multi-objective optimization and performance evaluation of refractory materials for high-temperature industrial furnaces, Journal of Advanced Materials Science 12(3) (2024) 234–248. https://doi.org/10.1177/16878132251346230

[42] L. Bouna, A. A. E. Fakir, Y. Ettahiri, H. Abara, A. Jada, K. Draoui, and M. Ezahri, "Understanding the impact of kaolinite/muscovite ratio in natural clays on oxide contents, physisorbed water, and structural water fractions," Materials Chemistry and Physics, vol. 314, no. 1, p. 128858, 2024, doi: 10.1016/j.matchemphys.2023.128858

[43] P. Manurung, E. S. Ginting, E. Ginting, and Suprihatin, "Synthesis and characterisation of nano-silica based on pumice using NaOH," Journal of Physical Science, vol. 33, no. 1, pp. 17–28, 2022. Available: https://doi.org/10.21315/jps2022.33.1.2

Received: 25/04/2026; Revised: 26/05/2026; Accepted: 29/05/2026; Published: 02/06/2026